# Soft Mathematical Morphology: Extensions, Algorithms and Implementations

A. Gasteratos and I. Andreadis

Laboratory of Electronics

Section of Electronics and Information Systems Technology

Department of Electrical and Computer Engineering

Democritus University of Thrace

GR-671 00 Xanthi, Greece

E-mail: {agaster, iandread}@demokritos.cc.duth.gr

# Preface

Linear filters have been used as the primary tools in signal and image processing. They exhibit many desirable properties, such as the superposition, which makes them easy to design and implement. Furthermore, they are the best solution in additive Gaussian noise suppression. However, when the noise is not additive or when there exist system non-linearities linear filters are not adequate. For example all image processing is, of necessity, non-linear. In such cases non-linear filters should be utilized. The advantage of non-linear filters is their ability to pass structural information while suppressing noise or removing clutter. Pattern and edge information are often crucial to image understanding, and in many circumstances it is possible to design non-linear filters that pass structural information in a manner superior to that of linear filters. Non-linear filtering has been developed along three lines: logical (set), geometrical (shape) and numerical (order based). These three approaches are deeply interrelated. Shape-based non-linear filtering is centered around mathematical morphology.

Soft morphological filters are a relatively new subclass of non-linear filters. They combine morphological filters with weighted order statistics filters. Standard morphological operators are defined using local min and max operations. In soft mathematical morphology rather flexible definitions are provided, by substituting the min and max operators with general weighted order statistics. Soft morphological filters have been introduced to improve the results of standard morphological filters in noisy conditions. In this paper the trends in soft mathematical morphology are described. Fuzzy soft mathematical morphology applies the concepts of soft morphology to fuzzy sets. The definitions of the basic fuzzy soft morphological operations and their algebraic properties are provided. An algorithm for soft morphological structuring element decomposition is

also presented. Furthermore, techniques for software and hardware implementation of soft morphological operations are included.

# Table of Contents

# I. Introduction

Mathematical morphology is an active and growing area of image processing and analysis. It is based on set theory and topology (Matheron, 1975, Serra, 1982, Haralick *et al*., 1986, Giardina and Dougherty, 1988). Mathematical morphology studies the geometric structure inherent within the image. For this reason it uses a predetermined geometric shape known as the structuring element. Erosion, which is the basic morphological operation, quantifies the way in which the structuring element fits into the image. Mathematical morphology has provided solutions to many tasks, where image processing can be applied, such as in remote sensing, optical character recognition, radar image sequence recognition, medical imaging etc. Soft mathematical morphology was introduced by Koskinen *et al.* (1991). In this approach the definitions of the standard morphological operations were slightly relaxed in such a way that a degree of robustness is achieved, while most of their desirable properties are maintained. Soft morphological filters are less sensitive to additive noise and to small variations in object shape than standard morphological filters. They have found applications mainly in noise removal, in areas such as medical imaging and digital TV (Harvey, 1998).

Another, relatively new, approach to mathematical morphology is fuzzy mathematical morphology. A fuzzy morphological framework has been introduced by Sinha and Dougherty (1992). In this framework the images are not treated as crisp binary sets, but as fuzzy sets. The set union and intersection have been replaced by fuzzy bold union and bold intersection, respectively, in order to formulate fuzzy erosion and dilation, respectively. This attempt to adapt mathematical morphology into fuzzy set theory is not unique. Several other attempts have been developed independently by researchers, and they are all described and discussed by Bloch and Maitre (1995). Several fuzzy

mathematical morphologies are grouped and compared and their properties are studied. A general framework, unifying all these approaches is also demonstrated.

In this paper recent trends in soft mathematical morphology are presented. The rest of the paper is organized as follows. The standard morphological operations and their algebraic properties and fuzzy morphology are discussed in section II. Soft mathematical morphology is described in section III. A soft morphological structuring element decomposition technique is introduced in section IV. The definitions of fuzzy soft morphological operations and their algebraic properties are provided in section V. Several implementations of soft morphological filters are analyzed in section VI. Concluding remarks are made in section VII.

# II. Standard Mathematical Morphology

The considerations for the structuring element used by Haralick *et al*. (1987) have been adopted for the basic morphological operations. Also, the notations of the extensions of the basic morphological operations (soft morphology, fuzzy morphology and fuzzy soft morphology) are based on the same consideration. Moreover, throughout the paper the discrete case is considered, i.e. all sets belong to the Cartesian grid $Z^2$.

## A. Binary Morphology

Let the set A denote the image under process and the set B the structuring element. Binary erosion and dilation are defined:

$$A \top B = \bigcap_{x \in B} (A)_{-x} \quad \text{and} \tag{1}$$

$$A \oplus B = \bigcup_{x \in B} (A)_x \tag{2}$$

respectively.

where A, B are sets of $Z^2$ and $(A)_x$ is the translation of A by $x$, which is defined as follows:

$$(A)_x = \{c \in Z^2 \mid c = a + x \text{ for some } a \in A\} \tag{3}$$

The definitions of binary opening and closing are:

$$A \circ B = (A \ominus B) \oplus B \text{ and} \tag{4}$$

$$A \bullet B = (A \oplus B) \ominus B \tag{5}$$

respectively.

## B. Basic Algebraic Properties

The basic algebraic properties of the morphological operations are provided in this section:

*Duality Theorem*

Erosion and dilation are dual operations:

$$(A \ominus B)^C = A^C \oplus B^S \tag{6}$$

where $A^C$ is the complement of A, and it is defined as:

$$A^C = \{x \in Z^2 \mid x \notin A\} \tag{7}$$

and $B^S$ is the reflection of B, and it is defined as:

$$B^S = \{x \mid \text{for some } b \in B,\ x = -b\} \tag{8}$$

Opening and closing are also dual operations:

$$(A \bullet B)^C = A^C \circ B^S \tag{9}$$

*Translation Invariance*

Both erosion and dilation are translation invariant operations:

$$(A)_x \oplus B = (A \oplus B)_x \quad \text{and} \tag{10}$$

$$(A)_x \ominus B = (A \ominus B)_x \tag{11}$$

respectively.

*Increasing*

Both erosion and dilation are increasing operations:

$$? \subseteq ? \Rightarrow ? \ominus C \subseteq ? \ominus C \tag{12}$$

$$? \subseteq ? \Rightarrow ? \oplus D \subseteq B \oplus D \tag{13}$$

*Distributivity*

Erosion distributes over set intersection and dilation distributes over set union:

$$(? \cap ?) \ominus C = (? \ominus C) \cap (? \ominus C) \text{ and} \tag{14}$$

$$(A \cup B) \oplus C = (A \oplus C) \cup (B \oplus C) \tag{15}$$

respectively.

*Anti-extensivity - Extensivity*

Erosion is an anti-extensive operation, provided that the origin belongs to the structuring element:

$$0 \in B \Rightarrow A \top B \subseteq ? \quad (16)$$

Similarly, dilation is extensive, if the origin belongs to the structuring element:

$$0 \in ? \Rightarrow ? \subseteq ? \oplus ? \quad (17)$$

*Idempotency*

Opening and closing are idempotent, i.e. their successive applications do not change further the previously transformed result:

$$A \circ B = (A \circ B) \circ B \text{ and} \quad (18)$$

$$A \bullet B = (A \bullet B) \bullet B \quad (19)$$

## C. Gray-scale Morphology with Flat Structuring Elements

The definitions of morphological erosion and dilation of a function $f: F \to Z$ by a flat structuring element (set) B are:

$$(f \top B)(x) = \min \{f(y) \mid y \in (B)_x\} \text{ and} \quad (20)$$

$$(f \oplus B)(x) = \max \{f(y) \mid y \in (B^S)_x\} \quad (21)$$

respectively.

where $x, y \in Z^2$ are the spatial coordinates and $F \subseteq Z^2$ is the domain of the gray-scale image (function).

## D. Gray-scale Morphology with Gray-scale Structuring Elements

The definition of erosion and dilation of a function $f: F \rightarrow Z$ by a gray-scale structuring element $g: G \rightarrow Z$ are:

$$(f \top g)(x) = \min_{y \in G} \{ f(x+y) - g(y) \} \text{ and} \tag{22}$$

$$(f \oplus g)(x) = \max_{\substack{y \in G \\ x-y \in F}} \{ f(x - y) + g(y) \} \tag{23}$$

respectively.

where $x, y \in Z^2$ are the spatial coordinates and $F, G \subseteq Z^2$, are the domains of the gray-scale image (function) and gray-scale structuring element, respectively.

## E. Fuzzy Morphology

In this paper the definitions introduced by Sinha and Dougherty (1992) are used. These are a special case of the framework presented by Bloch and Maitre (1995). In this approach, fuzzy mathematical morphology is studied in terms of fuzzy fitting. The fuzziness is introduced by the degree to which the structuring element fits into the image. The operations of erosion and dilation of a fuzzy image by a fuzzy structuring element having a bounded support, are defined in terms of their membership functions as follows:

$$\mu_{A \top B}(x) = \min_{y \in B}\left[\min\left[1, 1 + \mu_A(x+y) - \mu_B(y)\right]\right] = \min\left[1,\ \min_{y \in B}\left[1 + \mu_A(x+y) - \mu_B(y)\right]\right] \quad \text{and} \quad (24)$$

$$\mu_{A \oplus B}(x) = \max_{y \in B}\left[\max\left[0, \mu_A(x-y) + \mu_B(y) - 1\right]\right] = \max\left[0, \max_{y \in B}\left[\mu_A(x-y) + \mu_B(y) - 1\right]\right] \quad (25)$$

where $x, y \in Z^2$ are the spatial coordinates and $\mu_A$, $\mu_B$ are the membership functions of the image and the structuring element, respectively.

It is obvious from Eqs. (24) and (25) that the results of both fuzzy erosion and dilation have membership functions whose values are within the interval [0,1].

# III. Soft Mathematical Morphology

In soft morphological operations the maximum or the minimum operations, used in standard gray-scale morphology, are replaced by weighted order statistics. A weighted order statistic is a certain element of a list, the members of which have been ordered. Some of the members from the original unsorted list, participate with a weight greater than one, i.e. they are repeated more than once, before sorting (David, 1981, Pitas and Venetsanolpoulos, 1990). Furthermore, in soft mathematical morphology the structuring element B is divided into two subsets; the core $B_1$ and the soft boundary $B_2$.

## A. Binary Soft Morphology

The basic definitions of the binary soft erosion and dilation are (Pu and Shih, 1995):

$$(A\top[B_1,B_2,k])(x)=\{x\in A\mid (k\times Card[A\cap(B_1)_x]+Card[A\cap(B_2)_x]) \geq kCard[B_1]+Card[B_2]-k+1\} \quad \text{and} \qquad (26)$$

$$(A\oplus[B_1,B_2,k])(x)=\{x\in A\mid\left(k\times Card[A\cap(B_1^S)_x]+Card\left[A\cap(B_2^S)_x\right]\right)\geq k\} \qquad (27)$$

respectively.

where $k$ is called the order index, which determines the number of times that the elements of core participate into the result and Card[X] denotes the cardinality of set X, i.e. the number of the elements of X.

In the extreme case when the order index $k$=1 or, alternatively, $B=B_1$ ($B_2=\varnothing$) soft morphological operations are reduced to standard morphological operations.

*Example 1*: The following example demonstrates a case of soft binary dilation and erosion. The adopted coordinate system is (row, column). The arrows denote the origin of the coordinate system and its direction.

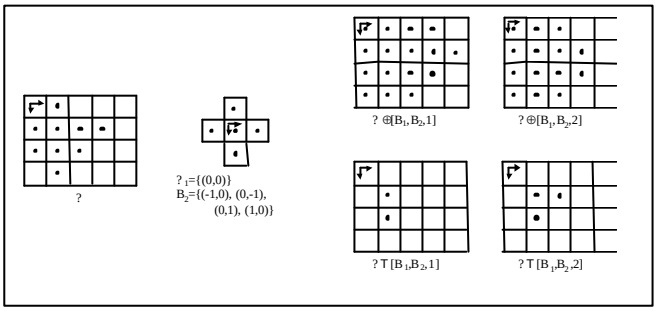


If $k$>Card[$B_2$], soft morphological operations are affected only by the core $B_1$, i.e. using $B_1$ as the structuring element. Therefore, in this case the nature of soft morphological operations is not preserved (Kuosmanen and Astola, (1995), Pu and Shih, (1995)). For this reason the constraint $k\leq \min\{Card(B)/2, Card(B_2)\}$ is used. In the above example min(Card(B)/2, Card($B_2$))=2.5 and, therefore, only the cases $k$=1 and $k$=2 are considered.

For $k$=1 the results of both dilation and erosion are the same to those that would have been obtained by applying Eqs. (2) and (1), respectively.

## B. Gray-scale Soft Morphology with Flat Structuring Elements

The definitions of soft morphology were first introduced by Koskinen *et al*. (1992), as transforms of a function by a set. In the definition of soft dilation the reflection of the structuring element is used, so that in the case of $k$=1 the definitions comply with (Haralick *et al.*, (1987)).

$$(f \top [B_1, B_2, k])(x) = \min^{(k)}(\{k \Diamond f(y) \mid y \in (B_1)_x\} \cup (\{f(z) \mid z \in (B_2)_x\}) \text{ and} \qquad (28)$$

$$(f \oplus [B_1, B_2, k])(x) = \max^{(k)}\left(\{k \Diamond (y) \mid y \in (B_1^S)_x\} \cup (\{f(z) \mid z \in (B_2^S)_x\}\right) \qquad (29)$$

respectively.

where $\min^{(k)}$ and $\max^{(k)}$ are the $k$th smallest and the $k$th largest element of the multiset, respectively; a multiset is a collection of objects, where the repetition of objects is allowed and the symbol $\Diamond$ denotes the repetition, i.e.: $\{k \Diamond f(x)\} = \{f(x), f(x), \ldots f(x)\}$ ($k$ times).

## C. Gray-scale Soft Morphology with Gray-scale Structuring Elements

Soft morphological erosion of a gray-scale image $f$: F→Z by a soft gray-scale structuring element $[a, ß, k]$: B→Z is (Pu and Shih, 1995):

$$f \top [a, ß, k](x) = \min_{\substack{y \in B_1 \\ z \in B_2}}^{(k)}(\{k \Diamond (f(x+y) - a(y))\} \cup \{f(x+z) - ß(z)\}) \qquad (30)$$

Soft morphological dilation of $f$ by $[a, ß, k]$ is:

$$f \oplus [a, ß, k](x) = \max_{\substack{(x-y),(x-z)\in F \\ y\in B_1 \\ z\in B_2}}{}^{(k)} \left(\{k\Diamond(f(x-y)+a(y))\} \cup \{f(x-z)+ß(z)\}\right) \quad (31)$$

where $x, y, z \in Z^2$, are the spatial coordinates; $a$: $B_1 \rightarrow Z$ is the core of the gray-scale structuring element; $ß$: $B_2 \rightarrow Z$ is the soft boundary of the gray-scale structuring element and $F, B_1, B_2 \subseteq Z^2$ are the domains of the gray-scale image, the core of the gray-scale structuring element and the soft boundary of the gray-scale structuring element, respectively.

Insert Figure 1 here →

Figure 1 demonstrates one-dimensional soft morphological operations and the effect of the order index $k$. The same structuring element is used for both operations. It is an one-dimensional structuring element with five discrete values. The central value corresponds to its core and it is equal to 30. Additionally it denotes the origin. The four remaining values belong to its soft boundary and they are equal to 20. From both Figures 1(a) and (b) it is obvious that the greater the value of the order index, the better the fitting.

## IV. Soft Morphological Structuring Element Decomposition

A soft morphological structuring element decomposition technique is described in this section (Gasteratos *et al*., 1998d). According to this technique, the domain B of the structuring element is divided into smaller non-overlapping sub-domains B1, B2, ... B*n*. Also, $B1 \cup B2 \cup ...Bn = B$. The soft morphological structuring elements obtain values from these domains and they are denoted by [?*1*, *µ1*, *k*], [?*2*, *µ2*, *k*], ... [?*n*, *µn*, *k*], respectively. These have common origin, which is the origin of the original structuring element. Additionally, the points of B which belong to its core are also points of the cores of B1, B2, ... B*n* and the points of B which belong to the soft boundary are also points of

the soft boundaries of B1, B2, ... B*n*. This process is graphically illustrated in Figure 2. In this figure the core of the structuring element is denoted by the shaded area.

Insert Figure 2 here →

Soft dilation and erosion are computed as follows:

$$f \oplus [a,ß,k](x) = \max_{i=1}^{n}{}^{(k)}[\max_{\substack{(x-y)\in B_1\\(x-z)\in B_2\\j=1}}^{k}{}^{(j)}(\{k\Diamond(f(x-y)+ ?_i(y))\}\cup\{f(x-z)+\mu_i(z)\})] \qquad (32)$$

$$f\top [a,ß,k](x) = \min_{i=1}^{n}{}^{(k)}[\min_{\substack{(x-y)\in B_1\\(x-z)\in B_2\\j=1}}^{k}{}^{(j)}(\{k\Diamond(f(x+y)- ?_i(y))\}\cup\{f(x+z)-\mu_i(z)\})] \qquad (33)$$

respectively.

where $B_1$ and $B_2$ are the domain of the core and the soft boundary of the large structuring element $[a, ß, k]$: $B \rightarrow Z$.

*Proof*:

$$\forall\, y\in B_1 : a(y) = \bigcup_{i=1}^{n} ?_i(y)$$

$$\Rightarrow f(x-y)+a(y) = \bigcup_{i=1}^{n}[f(x-y)+ ?_i(y)],\ (x-y)\in B_1$$

$$\Rightarrow k\Diamond(f(x-y)+a(y)) = k\Diamond\left(\bigcup_{i=1}^{n}[f(x-y)+ ?_i(y)]\right) = \qquad (34)$$
$$k\Diamond(f(x-y)+ ?_1(y),\ f(x-y)+ ?_2(y),\ldots f(x-y)+ ?_n(y)),(x-y)\in B_1$$

Also, $\forall\, z\in B_2 : ß(z) = \bigcup_{i=1}^{n}\mu_i(z)$

$$\Rightarrow f(x-z)+ß(z)=\bigcup_{i=1}^{n}[f(x-z)+\mu_i(z)]= \\ f(x-z)+\mu_1(z),\ f(x-z)+\mu_2(z),\ldots f(x-z)+\mu_n(z),\ \ (x\text{ - }z)\in \mathrm{B}_2 \tag{35}$$

Through Eqs. (31), (34) and (35) we obtain:

$$f\oplus[a,ß,k](x)=\max_{\substack{(x-y)\in \mathrm{B}_1\\(x-z)\in \mathrm{B}_2}}^{(k)}\begin{pmatrix}\{k\Diamond(f(x-y)+?_1(y),\ f(x-y)+?_2(y),\ldots f(x-y)+?_n(y))\}\cup\\ \{f(x-z)+\mu_1(z),\ f(x-z)+\mu_2(z),\ldots f(x-z)+\mu_n(z)\}\end{pmatrix}$$

$$=\max_{\substack{(x-y)\in \mathrm{B}_1\\(x-z)\in \mathrm{B}_2}}^{(k)}\begin{pmatrix}\{k\Diamond(f(x-y)+?_1(y))\}\cup\{f(x-z)+\mu_1(z)\},\\ \{k\Diamond(f(x-y)+?_2(y))\}\cup\{f(x-z)+\mu_2(z)\},\\ \ldots\\ \{k\Diamond(f(x-y)+?_n(y))\}\cup\{f(x-z)+\mu_n(z)\}\end{pmatrix}$$

$$=\max_{\substack{(x-y)\in \mathrm{B}_1\\(x-z)\in \mathrm{B}_2\\ i=1}}^{n,(k)}[\{k\Diamond(f(x-y)+?_i(y))\}\cup\{f(x-z)+\mu_i(z)\}]$$

The above equation can be expressed, in terms of order statistics of the multiset, as follows:

$$f\oplus[a,ß,k](x)=\max_{i=1}^{n,(k)}[\max_{\substack{(x-y)\in \mathrm{B}_1\\(x-z)\in \mathrm{B}_2}}^{(\mathrm{N})}(\{k\Diamond(f(x-y)+?_i(y))\}\cup\{f(x-z)+\mu_i(z)\}),$$
$$\max_{\substack{(x-y)\in \mathrm{B}_1\\(x-z)\in \mathrm{B}_2}}^{(\mathrm{N}-1)}(\{k\Diamond(f(x-y)+?_i(y))\}\cup\{f(x-z)+\mu_i(z)\}),$$
$$\ldots$$
$$\max_{\substack{(x-y)\in \mathrm{B}_1\\(x-z)\in \mathrm{B}_2}}(\{k\Diamond(f(x-y)+?_i(y))\}\cup\{f(x-z)+\mu_i(z)\})]$$

where N is the number of the elements of the multiset.

However, if an element is not greater than the local $(\mathrm{N}\text{-}k)^{\mathrm{th}}$ order statistic, then it cannot be greater than the global $(\mathrm{N}\text{-}k)^{\mathrm{th}}$ order statistic. Therefore, the terms $\max^{(\mathrm{N})}$ … $\max^{(k+1)}$ can be omitted:

$$f \oplus [a,ß,k](x) = \max_{i=1}^{n}{}^{(k)}[\max_{\substack{(x-y)\in B_1\\(x-z)\in B_2}}{}^{(k)}(\{k\Diamond(f(x-y)+ ?_i(y))\}\cup\{f(x-z)+\mu_i(z)\}),$$
$$\max_{\substack{(x-y)\in B_1\\(x-z)\in B_2}}{}^{(k-1)}(\{k\Diamond(f(x-y)+ ?_i(y))\}\cup\{f(x-z)+\mu_i(z)\}),$$
$$\ldots$$
$$\max_{\substack{(x-y)\in B_1\\(x-z)\in B_2}}(\{k\Diamond(f(x-y)+ ?_i(y))\}\cup\{f(x-z)+\mu_i(z)\})]$$

$$= \max_{i=1}^{n}{}^{(k)}[\max_{\substack{(x-y)\in B_1\\(x-z)\in B_2\\j=1}}^{k}{}^{(j)}(\{k\Diamond(f(x-y)+ ?_i(y))\}\cup\{f(x-z)+\mu_i(z)\})]$$

Similarly Eq. (33) can be proven.

*Example 2*: Let us consider the following image *f* and soft structuring element [*a, ß*]*:*

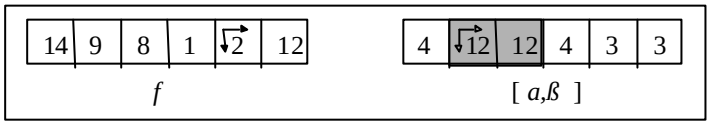


Soft dilation at point (0,0) for $k$=2, according to Eq. (31) is:

$$f \oplus [a,ß,2](0,0) = \max{}^{(2)}(\{2\Diamond(14,13)\}\cup\{16,12,12,17\}) = \max{}^{(2)}(14,14,13,13,16,12,12,17) = 16$$

According to the proposed technique the structuring is divided into three structuring elements:

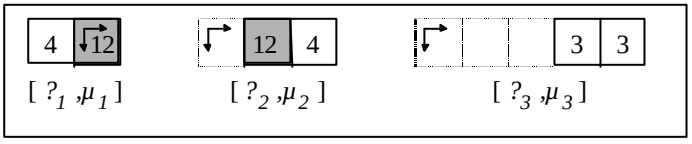


The following multisets are obtained from the above structuring elements:{2◊(14),16} , {2◊(13),12} and {12,17}, for the first the second and the third structuring elements, respectively. From these multisets the max and max$^{(2)}$ elements are retained: ({16,14},

{13,13} and {17,12}). The $\max^{(2)}$ of the union of these multisets, i.e. 16, is the result of soft dilation at point (0,0). It should be noticed that although 16 is the max of the first multiset, it is also the $\max^{(2)}$ of the global multiset.

# V. Fuzzy Soft Mathematical Morphology

## A. Definitions

Fuzzy soft mathematical morphology operations are defined taking into consideration that in soft mathematical morphology the structuring element is divided into two subsets, i.e. the core and the soft boundary, from which the core 'weights' more than the soft boundary in the formation of the final result. Also, depending on $k$, the $k$th order statistic provides the result of the operation. Also, fuzzy soft morphological operation should preserve the notion of fuzzy fitting (Sinha and Dougherty, 1992). Thus, the definitions for fuzzy soft erosion and fuzzy soft dilation are (Gasteratos *et al*., 1998a):

$$\mu_{A\top[B_1,B_2,k]}(x) = \min[1, \min_{\substack{y\in B_1\\ z\in B_2}}^{(k)} (\{k\Diamond(\mu_A(x+y) - \mu_{B_1}(y) + 1)\} \cup \{\mu_A(x+z) - \mu_{B_2}(z) + 1\})] \quad \text{and} \tag{36}$$

$$\mu_{A\oplus[B_1,B_2,k]}(x) = \max[0, \max_{\substack{y\in B_1\\ z\in B_2}}^{(k)} (\{k\Diamond(\mu_A(x-y) + \mu_{B_1}(y) - 1)\} \cup \{\mu_A(x-z) + \mu_{B_2}(z) - 1\})] \tag{37}$$

respectively.

where $x, y, z \in Z^2$, are the spatial coordinates and $\mu_A$, $\mu_{B_1}$, $\mu_{B_2}$ are the membership functions of the image, the core of the structuring element and the soft boundary of the

structuring element. Additionally, for the fuzzy structuring element $B \subset Z^2$: $B = B_1 \cup B_2$ and $B_1 \cap B_2 = \varnothing$.

It is obvious that for $k$=1 Eqs. (36) and (37) are reformed to Eqs. (24) and (25) respectively, i.e. standard fuzzy morphology.

*Example 3:* Let us consider the image A and the structuring element B. Fuzzy soft erosion and fuzzy soft dilation are computed for cases $k$=1 and $k$=2.

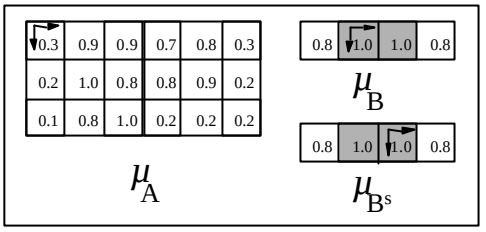


In order to preserve the nature of soft morphological operations, the constraint $k \le \min\{\mathrm{Card}(B)/2, \mathrm{Card}(B_2)\}$ is adopted in fuzzy soft mathematical morphology, as well as in soft mathematical morphology. In this example only the cases of $k$=1 and $k$=2 are considered, in order to comply with this constraint.

*Case 1* ($k$=1): The fuzzy soft erosion of the image is calculated as follows:

$$\mu_E(0,0) = \mu_{AT[B_1,B_2,1]}(0,0) = \min[1, \min[0.3-1+1, 0.9-1+1, 0.9-0.8+1]] = 0.3$$
$$\mu_E(0,1) = \min[1, \min[0.3-0.8+1, 0.9-1+1, 0.9-1+1, 0.7-0.8+1]] = 0.5$$
$$\vdots$$
$$\mu_E(5,2) = \min[1, \min[0.2-0.8+1, 0.2-1+1]] = 0.2$$

Therefore, the eroded image is:

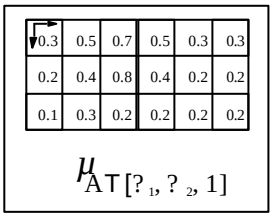


The values of the eroded image at points (0, 2) and (1, 2) are higher than the rest values of the image. This agrees with the notion of fuzzy fitting, since only at these points the

structuring element fits better than the rest points of the image. Fuzzy erosion quantifies the degree of structuring element fitting. The larger the number of pixels of the structuring element, the more difficult the fitting. Furthermore, fuzzy soft erosion shrinks the image. If fuzzy image A is considered as a noisy version of a binary image (Sinha and Dougherty, 1992), then the object of interest consists of points (0, 1), (0, 2), (0, 3), (0, 4), (1, 1), (1, 2), (1, 3), (1, 4), (2, 1) and (2, 2) and the rest is the background. By eroding the image with a 4pixel horizontal structuring element it would be expected that the eroded image would comprise points (0, 2) and (1,2). This is exactly what it has been obtained.

Similarly, the dilation of the image is calculated as follows:

$$\mu_D(0,0) = \mu_{A\oplus[B_1,B_2,1]}(0,0) = \max[0, \max[0.3+1-1, 0.9+0.8-1]] = 0.7$$
$$\mu_D(0,1) = \max[0, \max[0.3+1-1, 0.9+1-1, 0.9+0.8-1]] = 0.9$$
$$\vdots$$
$$\mu_D(5,2) = \max[0, \max[0.2+0.8-1, 0.2+1-1, 0.2+1-1]] = 0.2$$

Therefore, the dilated image is:

| | | | | | |
|---|---|---|---|---|---|
| 0.7 | 0.9 | 0.9 | 0.9 | 0.8 | 0.8 |
| 0.8 | 1.0 | 1.0 | 0.8 | 0.9 | 0.9 |
| 0.6 | 0.8 | 1.0 | 1.0 | 0.8 | 0.2 |

$\mu_{A\oplus[?_1, ?_2, 1]}$

As it can be seen, fuzzy soft dilation expands the image. In other words the dilated image includes the points of the original image and also points (0, 0), (0, 5), (1, 0), (1, 5), (2, 0), (2, 3) and (2, 4).

*Case 2* (*k*=2): The erosion of the image is calculated as follows:

$$\mu_E(0,0) = \mu_{AT[B_1,B_2,2]}(0,0) = \min\left[1, \min^{(2)}[0.3, 0.3, 0.9, 0.9, 1.1]\right] = 0.3$$
$$\mu_E(0,1) = \min\left[1, \min^{(2)}[0.5, 0.9, 0.9, 0.9, 0.9, 0.9]\right] = 0.9$$
$$\vdots$$
$$\mu_E(5,2) = \min\left[1, \min^{(2)}[0.4, 0.2, 0.2]\right] = 0.2$$

The eroded image for $k$=2 is:

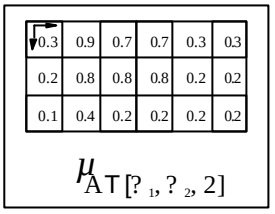


In this case the values of the eroded image at points (0, 1), (0, 2), (0, 3), (1, 1), (1, 2) and (1, 3) are higher than the rest values of the image. This is in agreement with the notion of fuzzy soft fitting. At these points the repeated $k$ times "high value" pixels, which are combined with the core of the structuring element and the pixels which are combined with the soft boundary of the structuring element, are greater than or equal to the $k\text{Card}[B_1]+\text{Card}[B_2]-k+1$.

Similarly, the dilation of the image is calculated:

$$\mu_D(0,0) = \mu_{A\oplus[B_1,B_2,2]}(0,0) = \max\left[0, \max^{(2)}[0.3, 0.3, 0.7]\right] = 0.3$$
$$\mu_D(0,1) = \max\left[0, \max^{(2)}[0.3, 0.3, 0.9, 0.9, 0.7]\right] = 0.9$$
$$\vdots$$
$$\mu_D(5,2) = \max\left[0, \max^{(2)}[0.4, 0.2, 0.2, 0.2, 0.2]\right] = 0.2$$

Therefore, the dilated image for $k$=2 is:

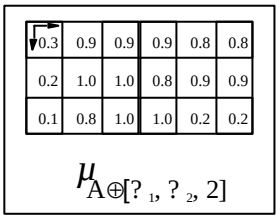


Here again fuzzy soft dilation expands the image, but more ‘softly’, than when $k$=1. This means that certain points ((0, 0),(1, 0), (2, 0) and (2, 4)) which were considered image points (when $k$=1), now ($k$=2) belong to the background. The greater the $k$, the less the effect of dilation.

Finally, fuzzy soft opening and closing are defined as:

$$\mu_{A\circ[B_1,B_2,k]}(x) = \mu_{(A\top[B_1,B_2,k])\oplus[B_1,B_2,k]}(x) \quad \text{and} \tag{38}$$

$$\mu_{A\bullet[B_1,B_2,k]}(x) = \mu_{(A\oplus[B_1,B_2,k])\top[B_1,B_2,k]}(x) \tag{39}$$

respectively.

Illustration of the basic fuzzy soft morphological operations is given through one-dimensional and two-dimensional signals. Figure 3 depicts fuzzy soft morphological erosion and dilation in one-dimensional space. More specifically, Figure 3a shows the initial one-dimensional signal and fuzzy soft erosion for $k$=1 and for $k$=2. Figure 3b shows the initial one-dimensional signal and fuzzy soft dilation for $k$=1 and for $k$=2. Figure 3c shows the structuring element. The core of the structuring element is the shaded area and the rest area of the structuring element is its soft boundary. From Figures 3a and 3b it becomes clear that the action of the structuring element becomes more effective when $k$=1, i.e. the results of both fuzzy soft erosion and dilation are more visible in the case of $k$=1, than in the case of $k$=2. Moreover, both erosion and dilation preserve the details of the original image better in the case of $k$=2, than in the case of $k$=1.

Insert Figure 3 here →

Figure 4 presents the result of fuzzy soft morphological erosion and dilation on a two-dimensional image. More specifically, Figures 4a and 4b present the initial image and the structuring element, respectively. The image in Figure 4b has been considered as an array of fuzzy singletons (Goetcharian, 1980). The results of fuzzy soft erosion ($k$=1) after the first and second interactions are presented in Figures 4c and 4d, respectively. The white area is reduced after each interaction. The white area of the eroded image (Figure 4c) is the area of the initial image, where the structuring element fits better. Similarly, Figures 4e and 4f present the results of fuzzy soft erosion ($k$=3) after the first and second interaction, respectively. Comparing Figures 4c and 4e it becomes clear that the greater the $k$ the less visible the results of fuzzy soft erosion. Figures 4g and 4h depict the results

of fuzzy soft dilation ($k=1$) after the first and second interaction, respectively. In the case of fuzzy soft dilation the white area increases. Similarly, in Figures 4i and 4j the results of fuzzy soft dilation ($k=3$) after the first and the second interaction, respectively. Again, the greater the $k$ the less visible the results of fuzzy soft dilation.

Insert Figure 4 here →

## B. Compatibility with Soft Mathematical Morphology

Let us consider *Example 3*. By thresholding image A and structuring element B (using a threshold equal to 0.5), the following binary image and binary structuring element are obtained:

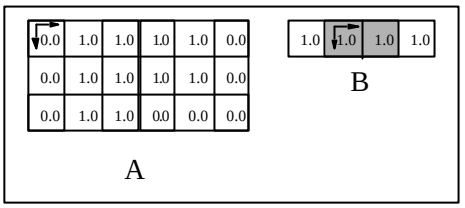


By applying soft binary erosion and soft binary dilation to image A with structuring element B the following images are obtained for $k=1$ and $k=2$:

$k=1$:

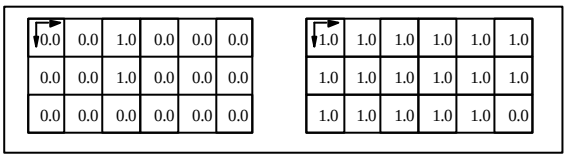


$k=2$:

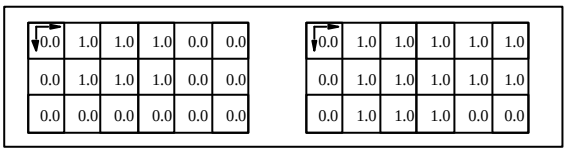


It is obvious that these results are identical to those of *Example 3*, when the same threshold value is used. This was expected, since binary soft morphology quantifies the soft fitting in a crisp way, whereas fuzzy soft erosion quantifies the soft fitting in a fuzzy way. The same results are obtained using a threshold equal to 0.55. However, when fuzzy soft morphology and thresholding with a threshold equal to or greater than 0.6 on the one hand and thresholding with the same threshold and soft morphology on the other hand are

applied, different results will be obtained. This means that, in general, the operations do not commute.

## C. Algebraic Properties of Fuzzy Soft Mathematical Morphology

*Duality Theorem*

Fuzzy soft erosion and dilation are dual operations:

$$\mu_{A^C \oplus [B_1, -B_2, k]}(x) = \mu_{(A \top [B_1, B_2, k])^C}(x) \tag{40}$$

Opening and closing are also dual operations:

$$\mu_{(A \bullet [B_1, B_2, k])^C}(x) = \mu_{A^C \circ [-B_1, -B_2, k]}(x) \tag{41}$$

*Translation Invariance*

Fuzzy soft erosion and dilation are translation invariant:

$$\mu_{(A)_u \top [B_1, B_2, k]}(x) = \left(\mu_{A \top [B_1, B_2, k]}(x)\right)_u \tag{42}$$

where $u \in Z^2$ .

*Increasing*

Both fuzzy soft erosion and dilation are increasing operations:

$$\mu_A < \mu_{A'} \Rightarrow \begin{cases} \mu_{A \top [B_1, B_2, k]}(x) < \mu_{A \top [B_1, B_2, k]}(x) \\ \\ \mu_{A \oplus [B_1, B_2, k]}(x) < \mu_{A' \oplus [B_1, B_2, k]}(x) \end{cases} \tag{43}$$

where A and A?, are two images with membership functions $\mu_{?}$ and $\mu_{A?}$, respectively and $\mu_{?}(x) < \mu_{A?}(x)$, $\forall x \in Z^2$.

*Distributivity*

Fuzzy soft erosion is not distributive over intersection, as it is in standard morphology:

$$\exists x \in Z^2 \text{and} \exists A1, A2, B \subseteq Z^2 \mid \mu_{(A1 \cap A2) \top [B_1, B_2, k]}(x) \neq \mu_{(A1 \top [B_1, B_2, k]) \cap (A2 \top [B_1, B_2, k])}(x) \quad (44)$$

*Example 4:* Consider the following image A and structuring element B, where image A is the intersection of images A1 and A2.

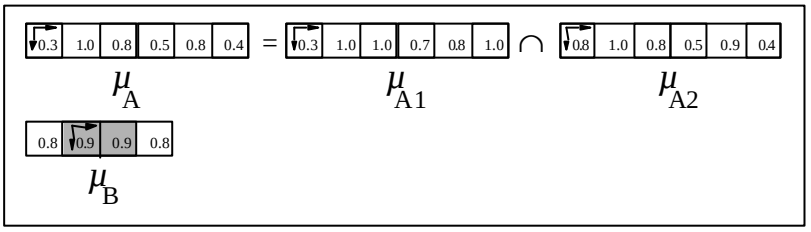


The fuzzy soft erosion for $k$=2 of A, A1, A2 and the intersection of the eroded A1 and the eroded A2 are:

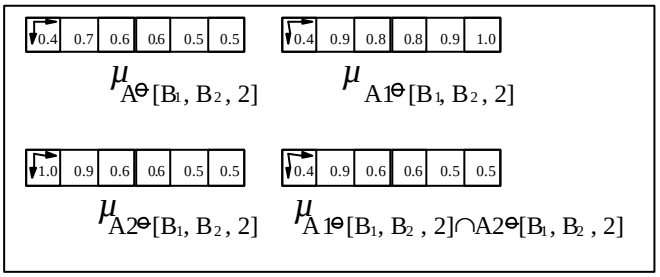


In general, fuzzy soft dilation does not distribute over union:

$$\exists x \in Z^2 \text{and} \exists A1, A2, B \subseteq Z^2 \mid \mu_{(A1 \cup A2) \oplus [B_1, B_2, k]}(x) \neq \mu_{(A1 \oplus [B_1, B_2, k]) \cup (A2 \oplus [B_1, B_2, k])}(x) \quad (45)$$

*Anti-extensivity - Extensivity*

Fuzzy soft opening is not anti-extensive. If it were anti-extensive, then $\mu_{A \circ [B_1, B_2, k]}(x) \leq \mu_A(x)$, $\forall x \in Z^2$. In the following example it is shown that $\exists x \in Z^2 \mid \mu_{A \circ [B_1, B_2, k]}(x) > \mu_A(x)$.

*Example 5*: Consider the image A and the structuring element B, for $k$=2. In this example $\mu_{A \circ [B_1, B_2, k]}(0,2) = 0.9 > \mu_A(0,2) = 0.2$,

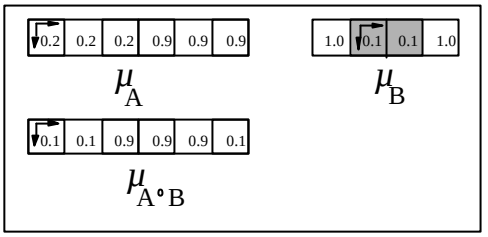


which means that fuzzy soft opening is not anti-extensive.

Similarly, it is shown that, in general, fuzzy soft closing is not extensive too: $\exists x \in Z^2$ and $A,B \subseteq Z^2 \mid \mu_{A \bullet [B_1, B_2, k]}(x) < \mu_A(x)$.

*Idempotency*

In general, fuzzy soft opening is not idempotent:

$$\exists x \in Z^2 \text{ and} \exists A, B \subseteq Z^2 \mid \mu_{A \circ [B_1, B_2, k]}(x) \neq \mu_{(A \circ [B_1, B_2, k]) \circ [B_1, B_2, k]}(x) \quad (46)$$

This is illustrated by the following example:

*Example 6:* Consider the image A and the structuring element B, for $k$=1.

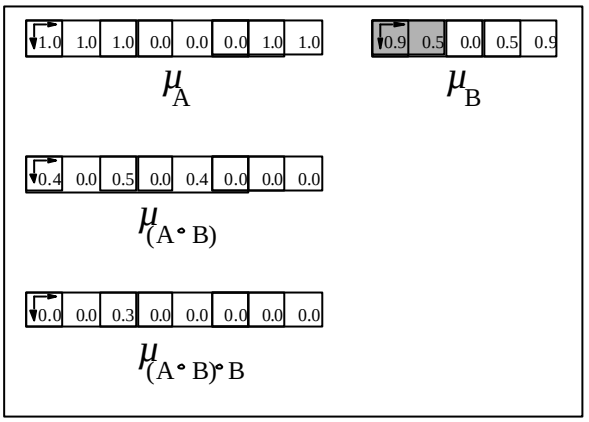


From this example it is obvious that fuzzy soft opening is not idempotent.

By the duality theorem (Eq. (41)) it can be proven that, in general, fuzzy soft closing is not idempotent too:

$$\exists x \in \mathrm{Z}^2 \text{ and} \exists \mathrm{A}, \mathrm{B} \subseteq \mathrm{Z}^2 \mid \mu_{\mathrm{A} \bullet [\mathrm{B}_1, \mathrm{B}_2, k]}(x) \neq \mu_{(\mathrm{A} \bullet [\mathrm{B}_1, \mathrm{B}_2, k]) \bullet [\mathrm{B}_1, \mathrm{B}_2, k]}(x) \qquad (47)$$

# VI. Implementations

Soft morphological operations are based on weighted order statistics and, therefore, algorithms such as mergesort and quicksort, which were developed for the computation of weighted order statistics, can be used for the computation of soft morphological filters (Kuosmanen and Astola, 1995). The average complexity of the quicksort algorithm is $O$(NlogN), where N is the number of elements to be sorted (Pitas and Venetsanopoulos, 1990). Therefore, the average complexity for a soft morphological operation utilizing a soft structuring element $[a, ß, k]:\mathrm{B} \rightarrow \mathrm{Z}$ is $O((k\mathrm{Card}[\mathrm{B}_1]+\mathrm{Card}[\mathrm{B}_2])\log(k\mathrm{Card}[\mathrm{B}_1]+\mathrm{Card}[\mathrm{B}_2]))$.

Hardware implementations of soft morphological operations include the threshold decomposition and the majority gate techniques. These structures along with an algorithm based on local histogram are described in some detail in this section.

## A. Threshold Decomposition

The threshold decomposition (Wendt *et al*., 1986) is a well-known technique for hardware implementation of non-linear filters. The implementation of soft morphological filters in hardware, using the threshold decomposition technique has been described in (Shih and Pu, 1995, Pu and Shih, 1995). According to this approach both the gray-scale image and the gray-scale structuring element are decomposed into $2^b$ binary images $f_i$ and $2^b$ structuring elements $ß_i$, respectively. Binary soft morphological operations are performed on the binary images by the binary soft structuring elements and then a maximum or a minimum selection at each position is performed, depending whether the operation is soft dilation or soft erosion, respectively. Finally the addition of the corresponding binary pixels is performed. Figure 5 demonstrates this technique for soft dilation.

Insert Figure 5 here →

The logic-gate implementation of binary soft morphological dilation and erosion are shown in Figures 6(a) and (b), respectively. The parallel counter counts the number of "ones" of the input signal and the comparator compares them to the order index $k$ and outputs one when this number is greater than or equal to $k$.

Insert Figure 6 here →

It is obvious that this technique, although it can achieve high-speed computation times, since it is realized using simple binary structures, it is hardware demanding. Its hardware complexity grows exponentially both with the structuring element size and the resolution of the pixels, i.e. its hardware complexity is $O(2^N 2^b)$.

## B. Majority Gate

### 1. Algorithm description

The majority gate algorithm is an efficient bit serial algorithm suitable for the computation of the median filter (Lee and Jen, 1992). According to this algorithm the MSBs of the numbers within the data window are first processed. The other bits are then processed sequentially until the less significant bits (LSBs) are reached. Initially, a set of signals (named the rejecting flag signals) are set to "1". These signals indicate which numbers are candidates to be the median value. If the majority of the MSBs is found to be "1", then the MSB of the output is "1", otherwise it is "0". The majority is computed through a CMOS programmable device, shown in Figure 7. In the following stage the bits of the numbers whose MSBs have been rejected by means of the rejecting flag signals are not taken into account. The majority selection procedure continues in the next stages until the median value is found.

Insert Figure 7 here →

Gasteratos et al. (1997a) have proposed an improvement of this algorithm for the implementation of any rank filter, using a single hardware structure. This is based on the concept that by having a method to compute the median value of 4N+1 numbers and by being able to control 2N of these numbers, any order statistic of the rest 2N+1 numbers can be determined. Suppose that there are W=2N+1 numbers $x_i$, the $r$-th order statistic of which is required. The 2N+1 inputs are the numbers $x_i$, whereas the rest are dummy inputs $d_l$ $(0 < l \leq 2N)$. The binary values of the dummy inputs can be either "00..0" or "11..1". This implies that when the W´ numbers are ordered in ascending sequence, $d_l$ are placed to the extremes of this sequence.

### 2. Systolic Array Implementation for Soft Morphological Filtering

#### a. A Systolic Array for a 3x3 Structuring Element

A pipelined systolic array capable of computing soft gray-scale dilation/erosion on a 3x3-pixel image window using a 3x3-pixel structuring element, both of 8-bit resolution, is presented in Figure 8 (Gasteratos *et al.*, 1998b). The central pixel of the structuring element is its core, whereas the rest eight pixels constitute its soft boundary. The inputs to this array are the 9 pixels of the image window, the 9 pixels of the soft morphological structuring element and a control signal MODE. Latches (L1) store the image window, latches (L*1) store the structuring element and latch (L**1) stores number $k$. Signal MODE is used to select the operation. When this is "1" soft dilation is performed, whereas when it is "0" soft erosion operation is performed. Image data is collected through multiplexers MUX1, which are controlled by the signal MODE. The pixels of the structuring element remain either unchanged for the operation of dilation or they are complemented (by means of XNOR gates) for the operation of erosion. In the next stage of the pipeline, data is fed into nine adders. In the case of soft erosion the 2's complements of the pixel values of the structuring element are added to the image pixel values. This is equivalent to the subtraction operation.

Insert Figure 8 here →

According to the constraint $k \leq \min\{\text{Card}(B)/2, \text{Card}(B_2)\}$, in this case $k$ is in the range $1 \leq k \leq 4$. Table 1 shows the number of the elements of the image data window, contained in the list, as well as the number of the dummy elements. For soft dilation all the dummy inputs are pushed to the top, whereas for soft erosion they are pushed to the bottom. Thus, the appropriate result is obtained from the order statistic unit. A control unit controls an array of multiplexers MUX2 (its input is number $k$). This is a decoder and its truth table is shown in Table 2. It provides the input to the order statistic unit, either a dummy number or a copy of the addition/subtraction result of the core.

Insert Table 1 here →

Insert Table 2 here →

The order statistic unit, consists of identical Processing Elements (PEs) separated by latches (L**4 to L**11). The resolution of the latches, which hold the addition/subtraction results or the dummy numbers (L3 to L11), decreases by one bit at

each successive stage, since there is no need to carry the bits, which have been already processed. On the other hand, the resolution of the latches which hold the result (L4* to L*11), increases by one bit at each successive stage. The circuit diagram of this PE is shown in Figure 9. In this Figure W'=4N+1; the 2N+1 inputs are the numbers $x_i$, whereas the rest are the dummy inputs. Due to its simplicity it can attain very sort processing times, independent of the data window size. Also, it becomes clear that the hardware complexity of the PE is linearly related to the number of its inputs.

Insert Figure 9 here →

b. Order Statistic Module Hardware Requirements for Other Structuring Elements

In this subsection a case study of the hardware requirements for the order statistic unit of a more complex structuring element is described. The arithmetic unit consists of a number of adders/subtractors equal to the number of pixels of the structuring element. Figure 10a illustrates the structuring element. In this case: Card(B)=16, Card($B_1$)=12, Card($B_2$)=4 and $k \leq \min\{8, 4\}$, i.e. $1 \leq k \leq 4$. When $k$=4 the maximum number of the elements of the multiset is Card($B_2$)+$k$Card($B_1$)=52. The 49th (4th) order statistic of the multiset is sought. Thus, the total number of the inputs to the order statistic unit is 97. The dummy numbers which are pushed to the top (bottom), in the operation of soft dilation (erosion), are 45. When $k$=3, the elements of the multiset are 40 and the 38th (3rd) order statistic is searched. Now the dummy numbers, which are pushed to the top (bottom), are 46 and to the bottom (top) are 11. In the same way, when $k$ =2 the elements of the multiset are 28 and the 27th (2nd) order statistic is searched and the dummy numbers which are pushed to the top (bottom) are 47 and to the bottom (top) are 22. Finally, when $k$=1 the elements of the multiset are 16 and the 16th (1st) order statistic is searched. In this case the dummy numbers which are pushed to the top (bottom) are 48 and to the bottom (top) are 33. For any structuring element an order statistic unit can be synthesized following the above procedure. In this case hardware complexity is linearly related both to the structuring element size and the resolution of the pixels, i.e. the hardware complexity is $O$(Nb).

Insert Figure 10 here →

3. Architecture for Decomposition of Soft Morphological Structuring Elements

An architecture suitable for the decomposition of soft morphological structuring elements is depicted in Figure 11. The structuring element is loaded into the *structuring element management* module. This divides the structuring element into $n$ smaller structuring elements and provides the appropriate one to the next stage. The pixels of the image are imported into the *image window management* module. This provides an image window, which interacts with the appropriate structuring element, provided by the *structuring element management* module. Both the previous modules consist of registers and multiplexers (MUXs), controlled by a counter mod$n$ (Figure 12). The second stage, i.e. the *arithmetic unit* consists of adders/subtractors (dilation/erosion) and an array of MUXs that are controlled by the order index $k$, as the one shown in Figure 9. The MUXs provide the multiple copies of the addition/subtraction results to the next stage, i.e. an array of *order statistic modules* (OSMs). The $\max^{(l)}/\min^{(l)}$ results ($l$=1,…$k$) of every multiset are collected through an *array of registers*. These registers provide the $n \times k$ $\max^{(l)}/\min^{(l)}$ of the $n$ multisets concurrently to the last stage OSM which computes the final result according to Eqs. (32) and (33).

Insert Figure 11 here →

Insert Figure 12 here →

## C. Histogram Technique

A method to compute an order statistic is by summing the values in the local histogram until the desired order statistic is reached (Dougherty and Astola, 1994). However, instead of adding the local histogram values serially, a successive approximation technique can be adopted (Gasteratos and Andreadis, 1999). This ensures that the result is traced in a fixed number of steps. The number of steps is equal to the number b of the bits per pixel. In successive approximation technique the result is computed recursively; in each step of the process the N pixel values are compared to a temporal result. Pixel values, which are

greater than, less than or equal to that temporal result, are marked with labels GT, LT and EQ, respectively. GT, LT and EQ are Boolean variables. Pixel labels are then multiplied by the corresponding pixel weight ($w_j$). The sum of LTs and EQs determines whether the $k$th order statistic is greater than, less than, or equal to the temporal values.

The pseudo-code of the algorithm follows:

*Notations:* N: Number of pixels; b: pixel value resolution (bits); $im_1$, $im_2$, … $im_N$: image pixels; $w_1$, $w_2$, … $w_N$: corresponding weights; $k$: the sought order statistic; temp: temporal result; $o$: output pixel.

**initial**

$o$=0

temp=$2^{b-1}$

**begin**

**for** $i$=1 **to** b **do**

**begin**

**compare**($im_1$, $im_2$, … $im_N$: temp)

{**if** $im_j$=temp **then** $EQ_j$=1 **else** $EQ_j$=0

**if** $im_j$<temp **then** $LT_j$=1 else $LT_j$=0}

**if** $\left(\sum_{j=1}^{N} w_j\left(EQ_j + LT_j\right) \geq k\right)$ AND $\left(\sum_{j=1}^{N} w_j LT_j < k\right)$

**then** $o \leftarrow$ temp

**elsif** $\sum_{j=1}^{N} w_j LT_j \geq k$

**then** temp $\leftarrow$ temp-$2^{b-1-i}$

**else** temp $\leftarrow$ temp+$2^{b-1-i}$

**end**

**end**

A module utilizing standard comparators, adders/subtractors, multipliers and multiplexers (for the "if" operations) can be used to implement this technique in hardware. Also, there are two ways to realize the algorithm. The first is through a loop, which feeds the temp signal back to the input b times. Such a module is demonstrated in Figure 13. Its inputs are the addition or subtraction results of the image pixel value data with the structuring element pixel values, depending on whether the operation is soft dilation or soft erosion, respectively. Alternatively, b successive modules can be used to process the data in a pipeline fashion. The latter implementation is more hardware demanding, but results into a faster hardware structure.

Insert Figure 13 here →

The above described algorithm requires a fixed number of steps equal to b. Furthermore, the number of steps grows linearly according to the pixel value resolution ($O$(b)). Its main advantage is that it can directly compute weighted rank order operations. This means that there is no need to reconstruct the local histogram according to the weights of the image pixels. Comparative experimental results using typical images, showed that for 5x5 and larger image data windows the combined local histogram and successive approximation technique outperforms the existing quicksort algorithm for weighted order statistics filtering (Gasteratos and Andreadis, 1999).

# VII. Conclusions

Soft morphological filters are a relatively new subclass of non-linear filters. They were introduced to improve the behavior of standard morphological filters in noisy environments. In this paper the recent descriptions of soft morphological image processing have been presented. Fuzzy soft mathematical morphology applies the concepts of soft morphology to fuzzy sets. The definitions and the algebraic properties have been illustrated through examples and experimental results. Techniques for soft morphological structuring element decomposition and its hardware implementation have been also described.

Soft morphological operations are based on weighted order statistics. Algorithms for implementation of soft morphological operations include the well-known mergesort and quicksort algorithms for weighted order statistics computation. An approach based on local histogram and a successive approximations technique has been also described. This algorithm is a great improvement in speed for 5x5 image data window or larger. Soft morphological filters can be implemented in hardware using the threshold decomposition and the majority gate techniques. The threshold decomposition technique is fast but its hardware complexity is exponentially related both to the structuring element size and the resolution of the pixels. In the majority gate algorithm the hardware complexity is linearly related both to the structuring element size and the resolution of the pixels.

# REFERENCES


1. Bloch, I., and Maitre, H. (1995). Pattern Recognition 28, 1341-1387.

2. David, H.A. (1981). "Order statistics" Wiley, New York.

3. Dougherty, E.R., and Astola, J. (1994). "Introduction to Nonlinear Image Processing" SPIE, Bellingham, Washington.

4. Gasteratos, A., and Andreadis, I. (1999). IEEE Signal Proc. Letters submitted.

5. Gasteratos, A., Andreadis, I., and Tsalides, Ph. (1997a). Pattern Recognition 30, 1571-1576.

6. Gasteratos, A., Andreadis, I., and Tsalides, Ph. (1998a). IEE Proceedings - Vision Image and Signal Processing 145, 40-49,

7. Gasteratos, A., Andreadis, I., and Tsalides, Ph. (1998b). IEE Proceedings - Circuits Devices and Systems 145, 201-206.

8. Gasteratos, A., Andreadis, I., and Tsalides, Ph. (1998d). In "Mathematical Morphology and its Applications to Image and Signal Processing" (H.J.A.M.

Heijmans, and J.B.T.M. Roerdink, eds), pp. 407-414, Kluwer Academic Publishers, Dordrecht, The Netherlands.

9. Giardina, C.R., and Dougherty, E.R. (1988). "Morphological Methods in Image and Signal Processing." Prentice-Hall, Englewood Cliffs, New Jersey.

10. Goetcharian, V. (1980). Pattern Recognition 12, 7-15.

11. Haralick, R.M., Sternberg, R., and Zhuang, X. (1986). IEEE Trans. Pattern Analysis and Machine Intelligence PAMI-9, 532-550.

12. Harvey, N.R. (1998). http://www.spd.eee.strath.ac.uk/~harve/bbc_epsrc.html.

13. Koskinen, L., Astola, J., and Neuvo, Y. (1991). Proc. SPIE Symp. Image Algebra and Morphological Image Proc. 1568, 262-270.

14. Kuosmanen, P., and Astola, J. (1995). J. Mathematical Imag. Vision 5, 231-262.

15. Lee, C.L., and Jen, C.W. (1992). IEE Proc. - G 139, 63-71.

16. Matheron, G. (1975). "Random Sets and Integral Geometry." Wiley, New York.

17. Pitas, I., and Venetsanopoulos, A.N. (1990). Proceedings of the IEEE 80, 1893-1921.

18. Pu, C.C., and Shih, F.Y. (1995). Graphical Models and Image Processing 57, 522-526.

19. Serra, J. (1982). "Image Analysis and Mathematical Morphology: Vol.I." Academic Press, London.

20. Shih, F.Y., and Pu, C.C. (1995). IEEE Trans. Signal Proc. 43, 539-544.

21. Shinha, D., and Dougherty, E.R. (1992). J. Visual Commun. Imag. Repres. 3, 286-302.

22. Wendt, P.D., Coyle, E.J., and Gallagher, N.C. Jr. (1985). IEEE Trans. Acoustics Speech and Signal Proc. ASSP-34, 898-911.

**Figure Captions**

**Figure 1.** Illustration of one-dimensional soft morphological operations and the effect of the order index $k$; (a) soft erosion and (b) soft dilation.

**Figure 2.** Example of a 4x4 soft morphological structuring element decomposition.

**Figure 3.** Illustration of one-dimensional fuzzy soft morphological operations and the effect of the order index $k$; (a) fuzzy soft erosion, (b) fuzzy soft dilation and (c) the structuring element.

**Figure 4.** (a) Image, (b) structuring element, (c) fuzzy soft erosion ($k=1$) after the first interaction, (d) fuzzy soft erosion ($k=1$) after the second interaction, (e) fuzzy soft erosion ($k=3$) after the first interaction, (f) fuzzy soft erosion ($k=3$) after the second interaction, (g) fuzzy soft dilation ($k=1$) after the first interaction, (h) fuzzy soft dilation ($k=1$) after the second interaction, (i) fuzzy soft dilation ($k=3$) after the first interaction and (j) fuzzy soft dilation ($k=3$) after the second interaction.

**Figure 5.** Illustration of the threshold decomposition technique for soft dilation.

**Figure 6.** Implementation of binary (a) soft morphological dilation and (b) soft morphological erosion.

**Figure 7.** Programmable CMOS majority gate.

**Figure 8.** Systolic array hardware structure implementing the majority gate technique for soft morphological filtering.

**Figure 9.** The basic processing element (PE).

**Figure 10.** (a) structuring element, (b) arrangement of the dummy numbers in soft morphological dilation using the structuring element of (a) and (c) arrangement of the dummy numbers in soft morphological erosion using the same structuring element.

**Figure 11.** Architecture for the implementation of the soft morphological structuring element decomposition technique.

**Figure 12.** Data window management for soft morphological structuring element decomposition.

**Figure 13.** Block diagram of a hardware module for the computation of weighted order statistics, based on the local histogram-successive approximation technique.

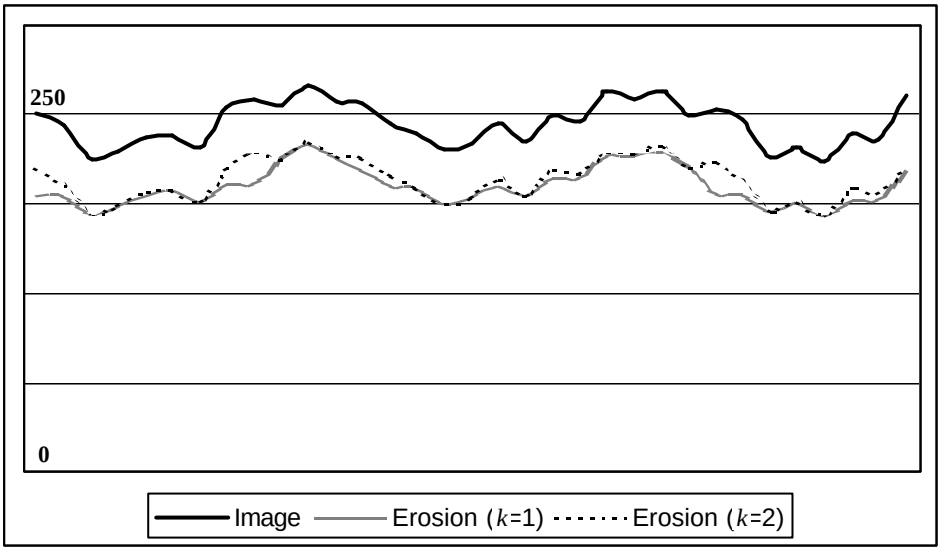
250
0
Image
Erosion (k=1)
Erosion (k=2)

(a)

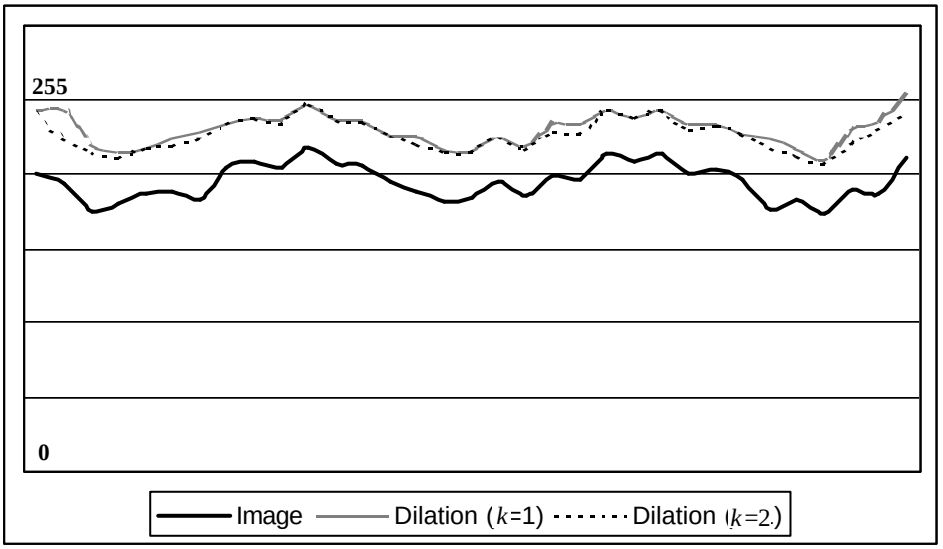
255
0
Image
Dilation (k=1)
Dilation (k=2)

(b)

**Figure 1.**

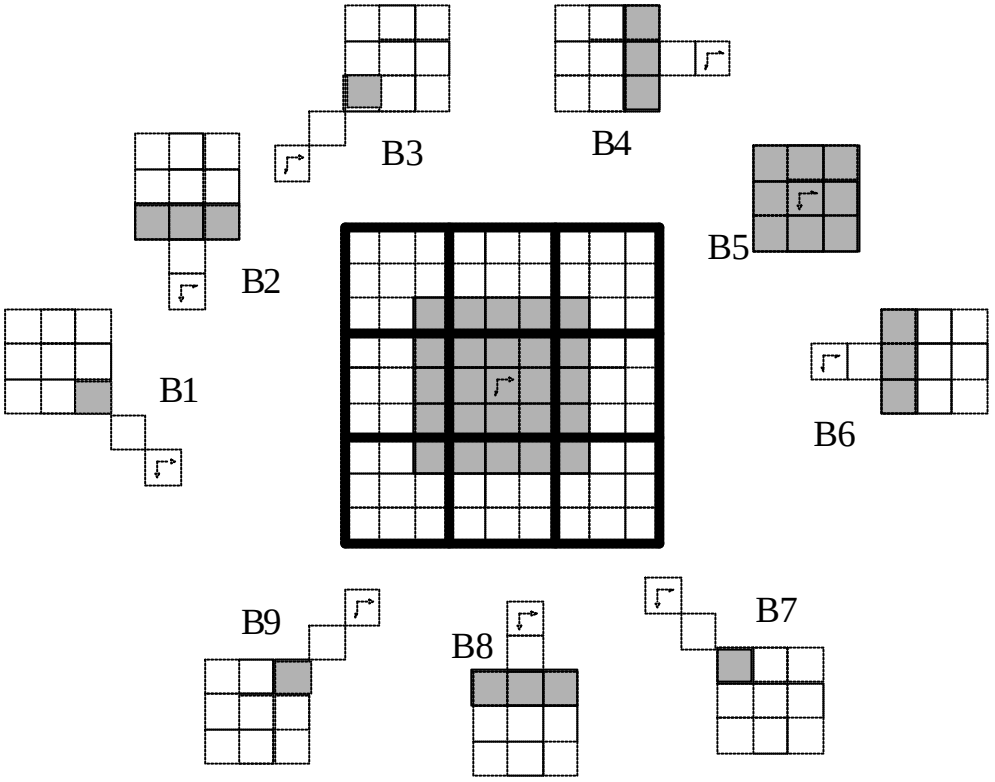


**Figure 2.**

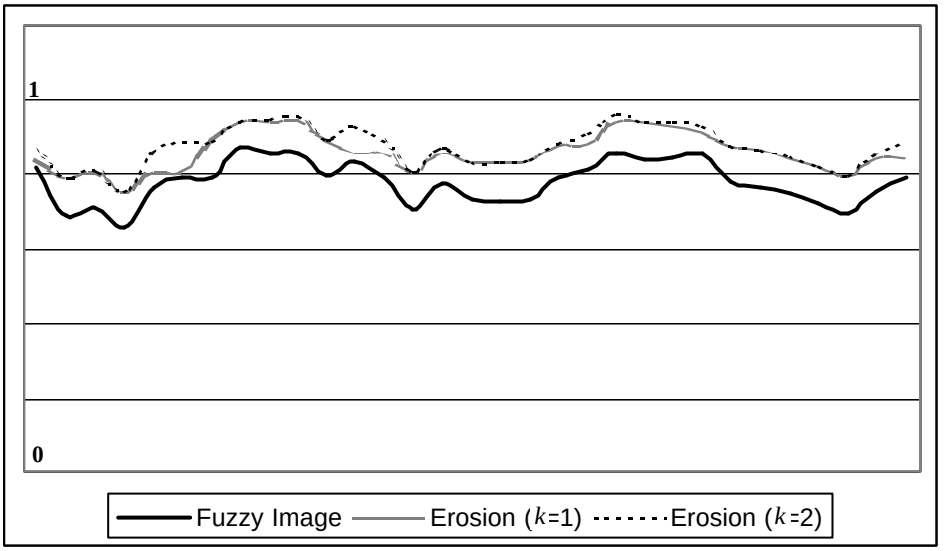
1
0
Fuzzy Image
Erosion (k=1)
Erosion (k=2)

(a)

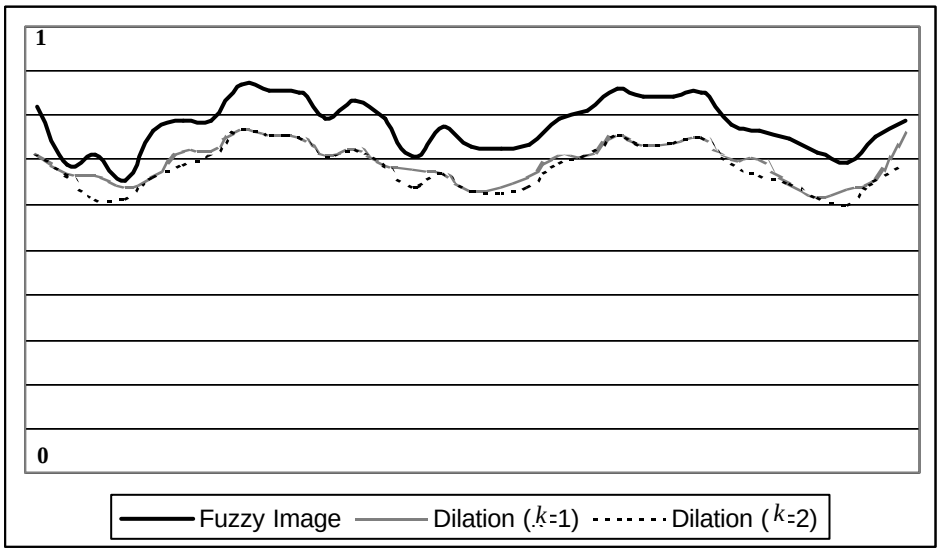
1
0
Fuzzy Image
Dilation (k=1)
Dilation (k=2)

(b)

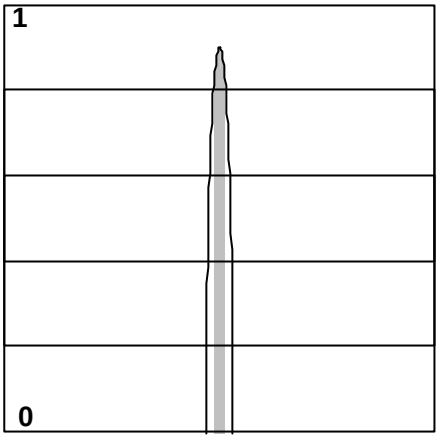


(c)

**Figure 3.**

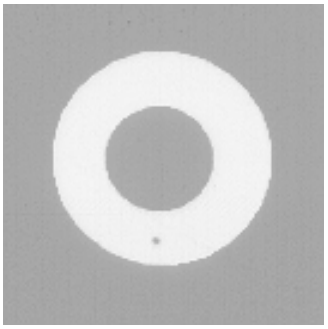

| | | | | |
|---|---|---|---|---|
| 1 | 1 | 1 | 1 | 1 |
| 1 | 1 | 1 | 1 | 1 |
| 1 | 1 | 1 | 1 | 1 |
| 1 | 1 | 1 | 1 | 1 |
| 1 | 1 | 1 | 1 | 1 |

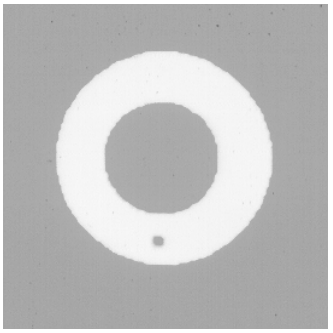

(a) (b) (c)

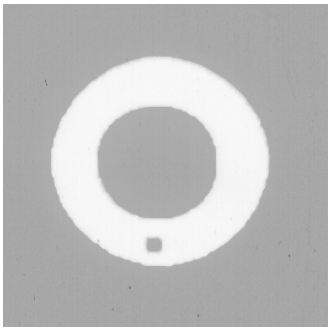

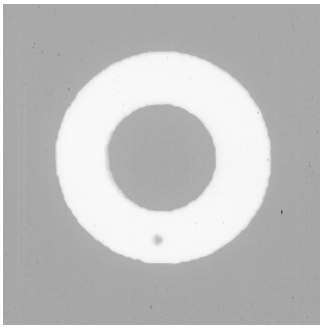

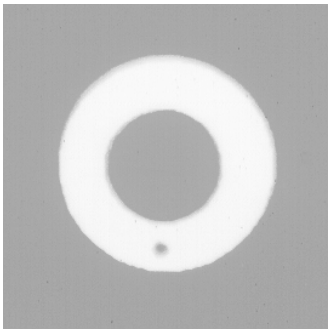

(d) (e) (f)

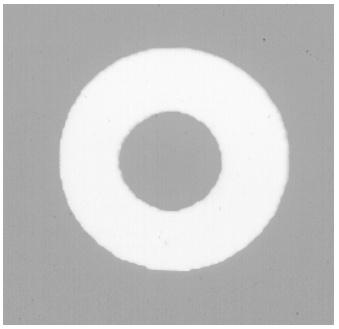

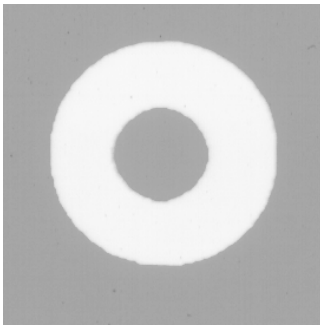

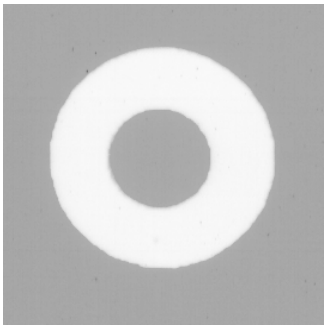

(g) (h) (i)

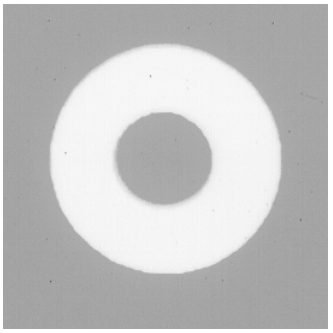

(j)

**Figure 4.**

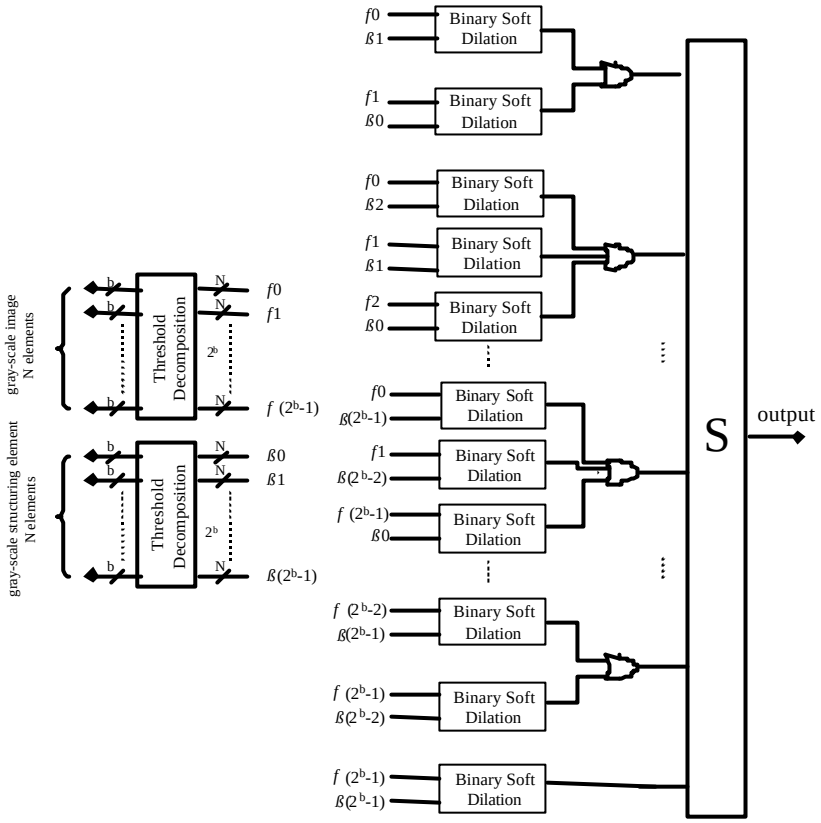
gray-scale image
N elements
gray-scale structuring element
N elements
b
N
Threshold
Decomposition
2^b
f0
f1
f (2^b-1)
ß0
ß1
ß(2^b-1)
Binary Soft
Dilation
f0
ß1
f1
ß0
f0
ß2
f1
ß1
f2
ß0
f0
ß(2^b-1)
f1
ß(2^b-2)
f (2^b-1)
ß0
f (2^b-2)
ß(2^b-1)
f (2^b-1)
ß(2^b-2)
f (2^b-1)
ß(2^b-1)
S
output

**Figure 5.**

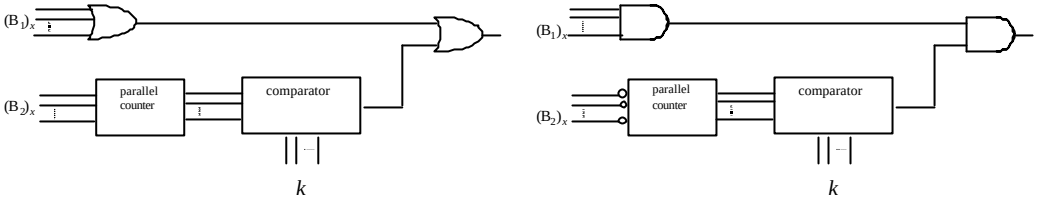
$(B_1)_x$
$(B_2)_x$
parallel counter
comparator
$k$
$(B_1)_x$
$(B_2)_x$
parallel counter
comparator
$k$

(a) (b)

**Figure 6.**

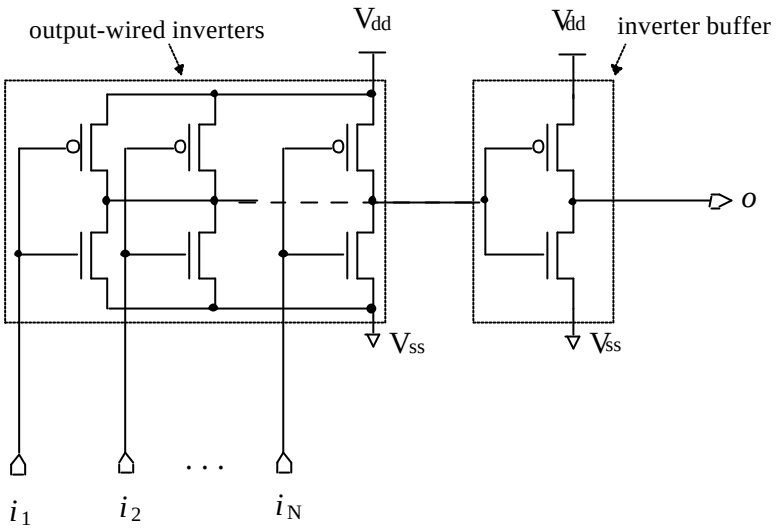


$i_1, i_2, \ldots i_N$ : inputs

$o$ : output

$V_{dd}$ , $V_{ss}$ : power supply

**Figure 7.**

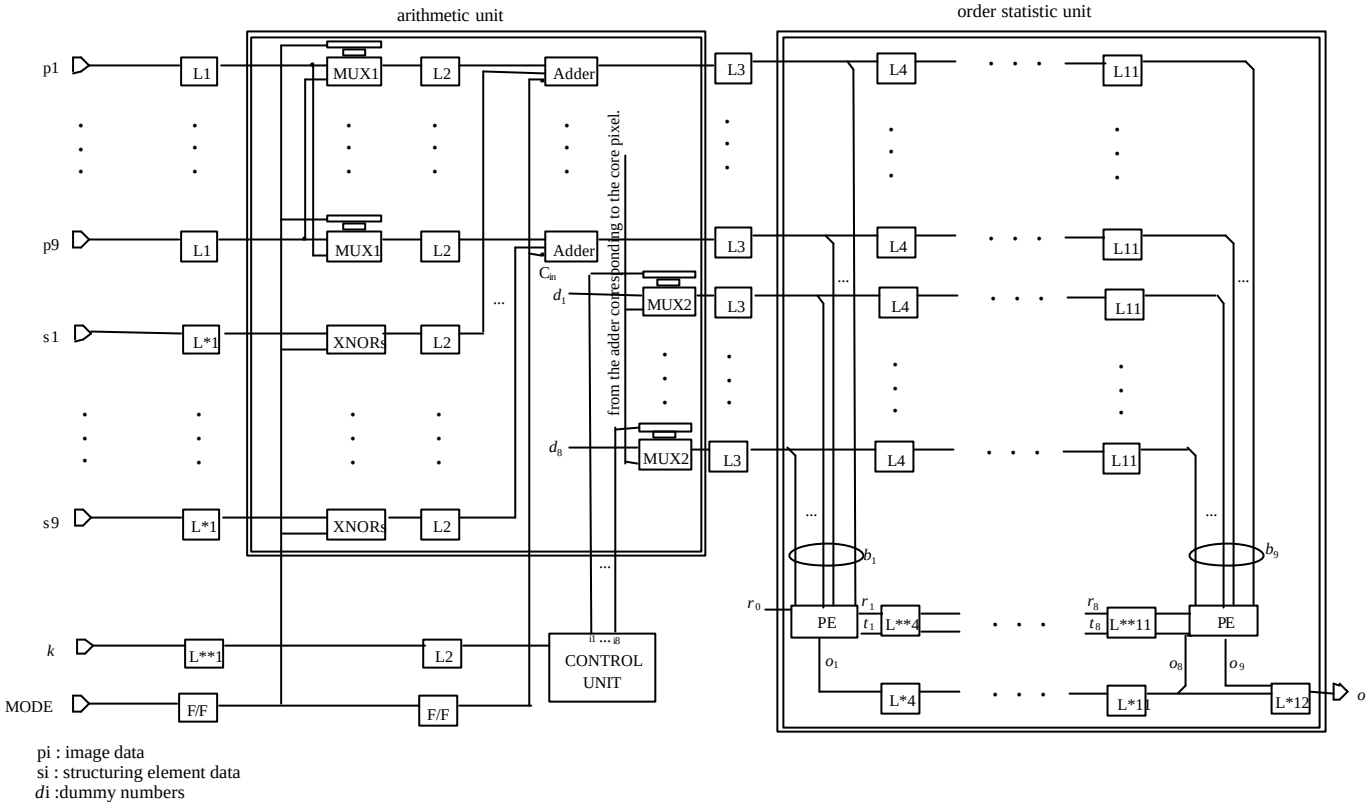
arithmetic unit
order statistic unit
p1
p9
s1
s9
k
MODE
L1
L*1
L**1
F/F
MUX1
XNORs
L2
Adder
L3
MUX2
from the adder corresponding to the core pixel.
CONTROL UNIT
L4
L*4
L11
L**11
L*11
L*12
PE
pi : image data
si : structuring element data
di :dummy numbers

**Figure 8.**

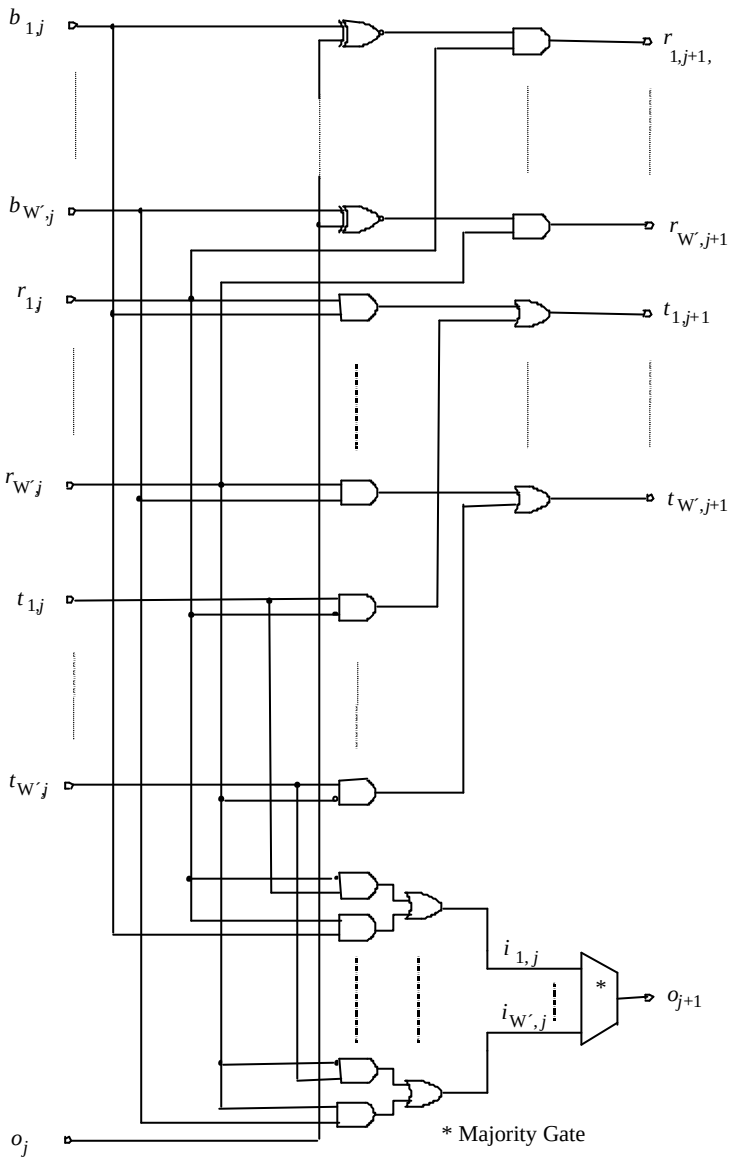


- $r_{i,j}$ the rejecting flag signals
- $t_{i,j}$ the setting flag signals
- $i_{i,j}$ intermediate signals
- $b_{i,j}$ the binary representation of the inputs

**Figure 9.**

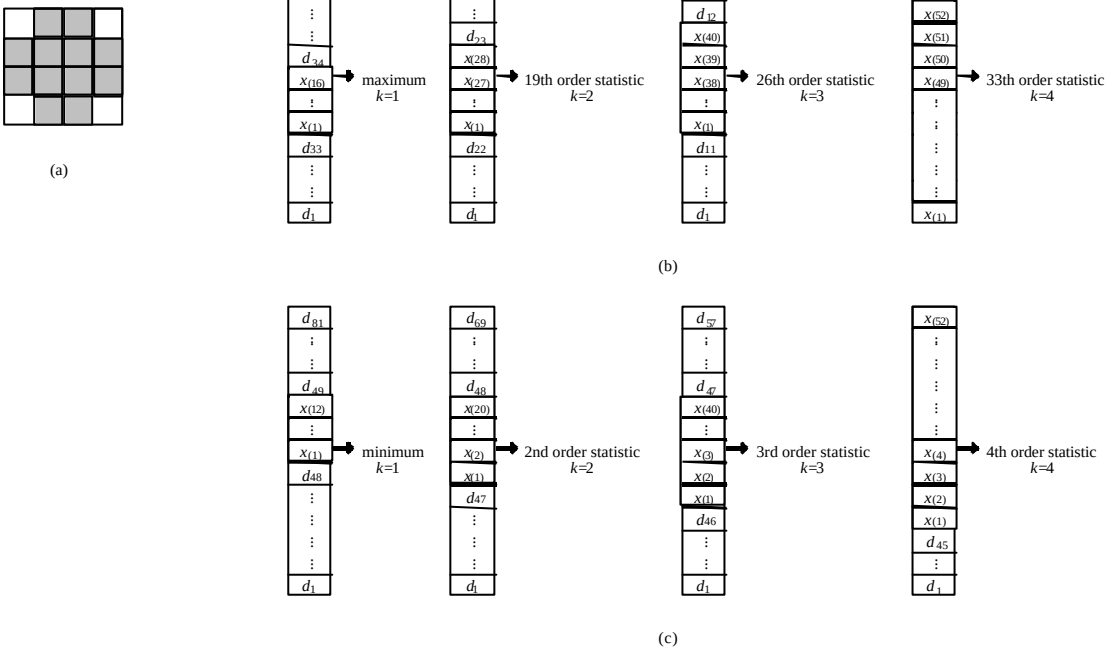
(a)
maximum
k=1
19th order statistic
k=2
26th order statistic
k=3
33th order statistic
k=4
(b)
minimum
k=1
2nd order statistic
k=2
3rd order statistic
k=3
4th order statistic
k=4
(c)

**Figure 10.**

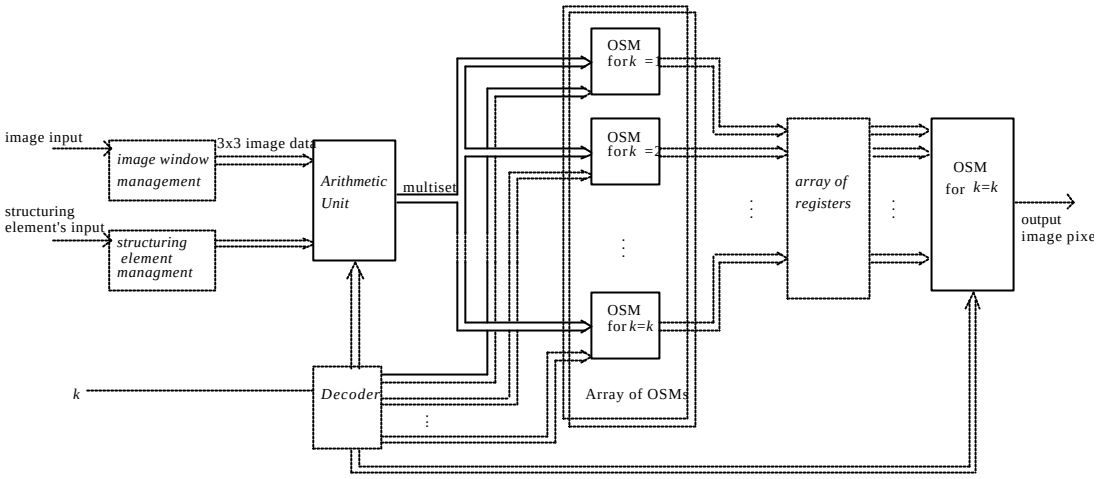
image input
image window management
3x3 image data
structuring element's input
structuring element managment
Arithmetic Unit
multiset
OSM for k =1
OSM for k =2
OSM for k=k
array of registers
OSM for k=k
output image pixe
k
Decoder
Array of OSMs

**Figure 11.**

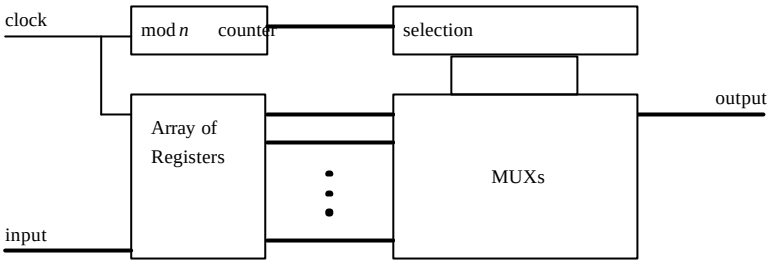
clock
mod n counter
selection
output
Array of
Registers
MUXs
input

**Figure 12.**

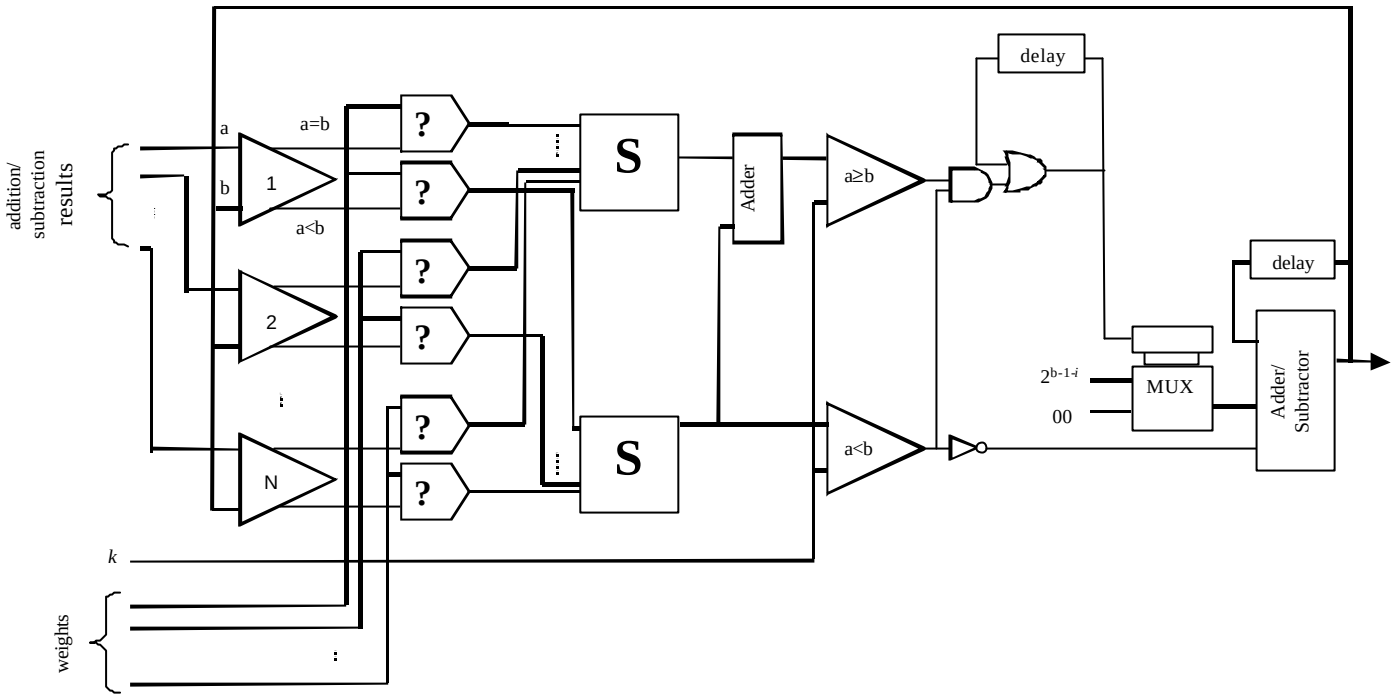
addition/
subtraction
results
a
b
a=b
a<b
1
2
N
?
S
Adder
a≥b
a<b
delay
delay
MUX
2b-1-i
00
Adder/
Subtractor
k
weights

**Figure 13.**

**Table Captions**

**Table 1.** Use of dummy numbers in the computation of weight order statistics.

**Table 2.** Truth table of the control unit.

**Table 1.**

| *k* | Sequence of numbers | Dummy numbers |
|---|---|---|
| 1 | 9 | 8 |
| 2 | 10 | 7 |
| 3 | 11 | 6 |
| 4 | 12 | 5 |

**Table 2.**

| **Input** | **Outputs** | | | | | | | |
|---|---|---|---|---|---|---|---|---|
| *k* | i1 | i2 | i3 | i4 | i5 | i6 | i7 | i8 |
| 0001 | 0 | 0 | 0 | 0 | 0 | 0 | 0 | 0 |
| 0010 | 1 | 0 | 0 | 0 | 0 | 0 | 0 | 0 |
| 0011 | 1 | 1 | 0 | 0 | 0 | 0 | 0 | 0 |
| 0100 | 1 | 1 | 1 | 0 | 0 | 0 | 0 | 0 |